Electronic and structural anomalies in lead chalcogenides

Su-Huai Wei and Alex Zunger
National Renewable Energy Laboratory, Golden, Colorado 80401
(Received 25 February 1997)

The rocksalt-structure PbS, PbSe, and PbTe semiconductors and their alloys exhibit a series of electronic-structure anomalies relative to the II-VI system, including the occurrence of direct gaps at the L point, anomalous order of band gaps and valence-band maximum energies versus anions, negative optical bowing, and negative band-gap pressure coefficients. We show that these anomalies result from the occurrence of the Pb s band below the top of the valence band, setting up coupling and level repulsion at the L point. Furthermore, we find that the topology of the frustrated octahedral structure leads to the occurrence in the random alloy of two distinct bonds for each anion-cation pair and to the predicted stabilization of *bulk* ordered Pb_2STe CuPt-like phase. [S0163-1829(97)05120-5]

I. INTRODUCTION

The rocksalt-structure lead chalocenide narrow-gap semiconductors PbS, PbSe, PbTe, and their alloys have been applied in long-wavelength imaging,[1] diode lasers,[2] and in thermophotovoltaic energy converters.[3] A close examination shows that these systems possess some peculiar electronic and structural properties relative to the more conventional zinc-blende II-VI and III-V compounds and alloys.

(i) Both the valence-band maximum (VBM) and the conduction-band minimum (CBM) states occur[4] at the L point in the Brillouin zone, while the direct gap in II-VI semiconductors occurs at the Γ point.[5]

(ii) The order[6,7] of the band gaps $E_g(\mathrm{PbS}) > E_g(\mathrm{PbTe}) > E_g(\mathrm{PbSe})$ is anomalous: in II-VI semiconductors the band gaps decrease monotonically with the anion's atomic number.[5]

(iii) The measured band offsets[8,9] suggest the order $E_{\mathrm{VBM}}(\mathrm{PbS}) > E_{\mathrm{VBM}}(\mathrm{PbSe}) > E_{\mathrm{VBM}}(\mathrm{PbTe})$, whereas measured and calculated offsets[10,11] in II-VI semiconductors show precisely a reversed order.

(iv) The band gaps have negative pressure coefficients,[12,13] i.e., they *decrease* as pressure is applied, in contrast to the behavior of the analogous transitions in[5] III-V and II-VI semiconductors.

(v) The band gap $E_g(x)$ of an $A_{1-x}B_x$ semiconductor alloy can usually be represented by $E_g(x) = (1-x)E_g(A) + xE_g(B) - bx(1-x)$, where b is the optical bowing coefficient. For all direct-gap zinc-blende semiconductor alloys the bowing coefficient[5] $b > 0$. For $PbSe_xTe_{1-x}$, however, a negative bowing is observed.[14,15]

(vi) Extended x-ray-absorption fine-structure measurements[16] revealed that Te-rich PbS_xTe_{1-x} alloys have *two* distinct Pb-S bonds with different lengths, in contrast with III-V and II-VI zinc-blende alloys where a single bond for each anion-cation pair is observed.[17]

Using a first-principles all-electron method, we show that the seemingly unrelated electronic anomalies (i)–(v) noted above have a common origin: they can be explained by noting that the Pb $6s$ band lies *below* the top of the valence band, while in conventional II-VI and III-V semiconductors the cation s band is unoccupied. The existence of an occupied-cation s band leads to strong level-repulsion between the valence states at the L point of the rocksalt Pb chalcogenide Brillouine zone. We further find that the topological properties of octahedral coordination lead to the occurrence in the random alloy of *two* distinct bonds for each anion-cation pair, and to the predicted stabilization of ordered $(\mathrm{Pb}X)_1(\mathrm{Pb}Y)_1$ $\langle 111 \rangle$ (''rocksalt CuPt'') structure.

II. METHOD OF CALCULATION

The band-structure calculation is performed using the local-density approximation (LDA) as implemented by the general-potential linearized augmented plane-wave (LAPW) method.[18] We used the Ceperley-Alder exchange-correlation potential as parametrized by Perdew and Zunger.[19] The core states are calculated fully relativistically, whereas the valence states are calculated scalar-relativistically and the spin-orbit interaction is added through a second variation procedure. To correct for the LDA error in the band gaps, a constant potential is applied to the conduction-band states, so as to match the calculated band gaps with the experimental data.[4] Table I gives the calculated lattice constants a_{eq}, bulk moduli B, and pressure derivatives of the bulk moduli B'. The calculated lattice constants and bulk moduli are in good agreement with the experimental data.[4]

The random $\mathrm{Pb}X_xY_{1-x}$ (X,Y = S, Se, or Te) alloys are described using the ''special quasirandom structures'' (SQS) approach.[20] In this approach, the alloy is modeled by occupying the anion sites in a supercell with X and Y atoms so that the first few structural-correlation functions are matched to the exact values in an *infinite* random alloy. Atoms in the SQS cell are fully relaxed by displacing them until the quantum-mechanical forces vanish.

The valence-band offset $\Delta E_v(\mathrm{Pb}X/\mathrm{Pb}Y)$ at an interface between two Pb chalcogenides PbX and PbY is calculated using the same procedure[10,11] as in photoemission core-level spectroscopy measurements. We calculated band offsets for both unstrained and coherently strained interfaces. The uncertainty in the calculated offsets is estimated to be less than 0.1 eV.

TABLE I. Calculated lattice constants a_{eq}, bulk moduli B, and pressure derivative of bulk moduli B' for the three Pb compounds. Results are compared with available experiment data compiled in Ref. 4.

	PbS		PbSe		PbTe	
Property	Calc.	Expt.	Calc.	Expt.	Calc.	Expt.
a_{eq} (Å)	5.906	5.929	6.098	6.117	6.439	6.443
B (Gpa)	66.3	53–70	60.8	41–61	51.7	40
B'	4.38		4.56		4.52	

III. RESULTS AND DISCUSSION

Figure 1 depicts relativistic band structures of PbS, PbSe, and PbTe, while Fig. 2 compares band structures of PbSe calculated scalar-relativistically (a) and fully relativistically (b). Table II gives some important band-structure parameters discussed in the following sections. Figures 1 and 2 show that the band structure of rocksalt PbX is distinguished from that of the zinc-blende II-VI and III-V semiconductors by having a Pb s band (dashed lines in Figs. 1 and 2) inside the valence band. This leads to strong-level repulsion at the L point between the two equal symmetry L_{1v} states [Fig. 2(a)]: the lower one being predominantly Pb s and the upper one being anion p. The electronic structure anomalies noted in the Introduction can be explained as follows.

(a) Why does the VBM occur at the L point? Of the high-symmetry states that could become the VBM (L_{1v}, L_{3v}, Γ_{15v}, $X_{4'v}$, $X_{5'v}$, see Fig. 2), only the $L_{1v}^{(1)}$ (we chose the cation sites as origin) has a counterpart inside the valence band with the same symmetry ($L_{1v}^{(2)}$ at ~ -9 eV). Since states with the same symmetry repel (in inverse proportion to their energy separation and in direct proportion to the coupling strength), the higher of the two L_{1v} states ($L_{1v}^{(1)}$) becomes the VBM. On the other hand, the valence states at Γ and X have equal symmetry counterparts only in the *conduction band* (e.g., Γ_{15v} with Γ_{15c}), so they are repelled *downwards*, being thus removed from the competition to become the VBM.

(b) Why does the CBM occur at the L point? Of the high-symmetry states that could become the CBM, the states at Γ (Γ_{15c}) and X ($X_{4'c}$, $X_{5'c}$) are repelled *upwards*, thus being removed from competition to become CBM. On the other hand, at the L point, $L_{2'c}$ is pushed down by (equal-symmetry) higher-lying conduction states. This is further enhanced by the spin-orbit coupling: once the spin-orbit interaction is turned on, the $L_{2'c}$ derived L_{6^-} state is pushed downwards by the equal-symmetry $L_{3'c}$ derived L_{6^-} state, thus becoming the CBM.

(c) Why do the band gaps have the order $E_g(PbS) > E_g(PbTe) > E_g(PbSe)$? Sulphur has the deepest p-orbital energy among the three chalcogen anions: the calculated LDA atomic valence p-orbital energies are -7.2, -6.7, and -6.2 eV for S, Se, and Te, respectively. Thus, in the absence of level repulsion, the VBM of PbX will be the deepest. Opposing this effect is the fact that PbS also has the largest p-s repulsion in the three PbX compounds. This results from the closeness of the energy of the S p orbital to the Pb s-orbital energy and from the shortness of the Pb-S bond. Due to this opposing effect, the energy spread of the L_{6^+} VBM state in the three Pb compounds is compressed relative to the spread of the free-atom p-orbital energies and can even reverse the order [see item (*d*) below]. A similar ''balancing act'' exists in the conduction bands: Although Te has the highest s-orbital energies (the calculated LDA atomic s-orbital energies are -17.4, -17.6, and -15.3 eV for S, Se, and Te, respectively), the closeness in energy between the $L_{3'c}$, and $L_{2'c}$ in PbTe (Table II, line 3) also causes a large repulsion between the equal symmetry $L_{6^-}(L_{3'c})$ and $L_{6^-}(L_{2'c})$ states through the spin-orbit coupling, pushing the $L_6(L_{2'c})$down (Table II, line 4). The net effect of these ''balancing acts'' is that all three compounds have similar

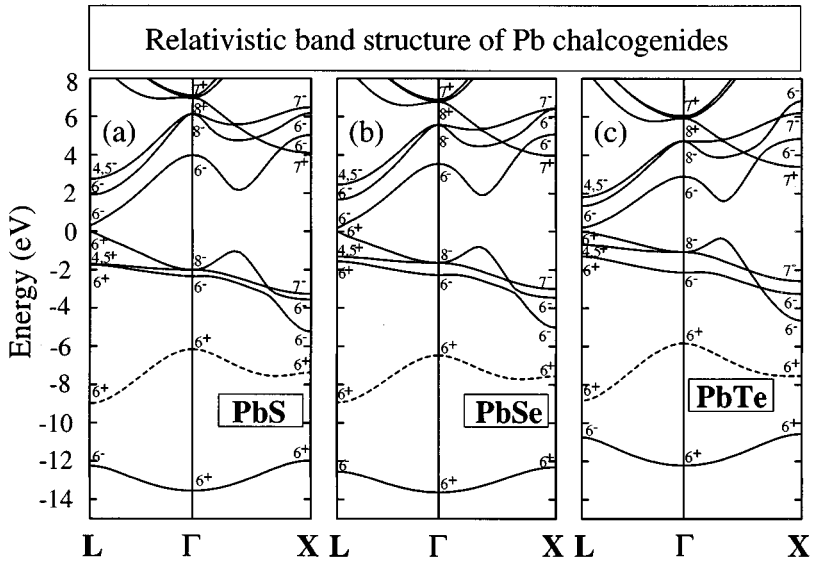

FIG. 1. Calculated relativistic electronic band structure of (a) PbS, (b) PbSe, and (c) PbTe. Origin of the coordination is at the cation site. The occupied Pb 6s bands are denoted by the dashed lines. The valence-band maximum is at zero.

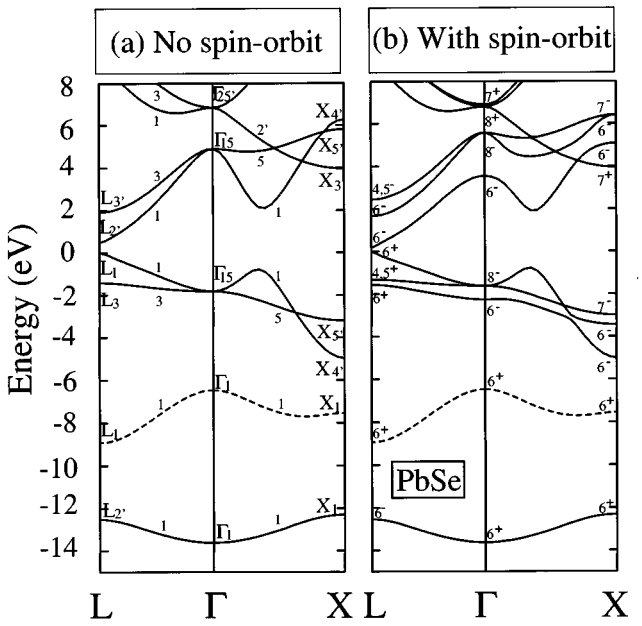

FIG. 2. Calculated electronic band structure of PbSe. (a) Semirelativistic (using single-space group notation), and (b) relativistic (using double-space group notation). Origin of the coordination is at the cation site. The occupied Pb 6*s* bands are denoted by the dashed lines. The valence-band maximum is at zero.

band gaps with $E_g(\mathrm{PbS}) > E_g(\mathrm{PbTe}) > E_g(\mathrm{PbSe})$ (Table II, line 1). On the other hand, no level repulsion exists at the Γ point, hence, the band gaps at Γ have the ''normal'' order of $E_g^{\Gamma}(\mathrm{PbS}) > E_g^{\Gamma}(\mathrm{PbSe}) > E_g^{\Gamma}(\mathrm{PbTe})$ (Fig. 1 and Table II, line 2).

(d) Why do the VBM's have the order $E_v(PbS) > E_v(PbSe) > E_v(PbTe)$? Since the VBM L_{1v} is mainly an anion *p* state, given the order of *p*-orbital energies of S, Se, and Te one would expect the VBM energies of Pb*X* to follow the order $E_v(\mathrm{PbTe}) > E_g(\mathrm{PbSe}) > E_g(\mathrm{PbS})$, just as is the case in II-VI compounds.[10,11] However, due to the strong anion *p* and Pb *s* coupling between the two L_{1v}, which pushes the L_{1v} VBM of PbS upwards more than in PbTe, the order of the VBM is reversed to $E_v(\mathrm{PbS}) > E_g(\mathrm{PbSe}) > E_g(\mathrm{PbTe})$. Since there is no *p*-*s* coupling at the Γ point, the top of the valence band at Γ is normal (see Table II, line 5 and Fig. 1).

Figure 3 shows our quantitatively calculated band offsets.

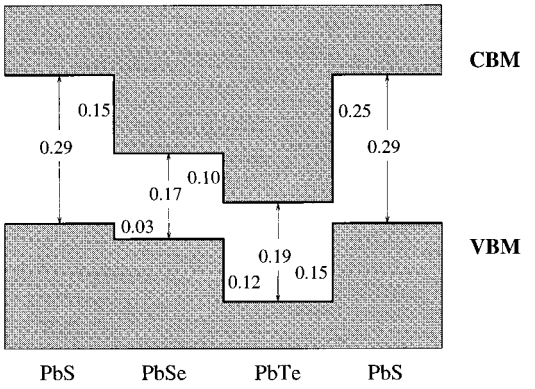

FIG. 3. Calculated unstrained-band alignment of PbS, PbSe, and PbTe. The conduction-band offsets are obtained using the relation $\Delta E_c = \Delta E_g + \Delta E_v$, where ΔE_g is the difference of measured band gaps.

We see that all the three interfaces have a type-II band alignment. Using Cr^{2+} impurity level as reference energy, the measured[8] valence-band offsets for PbTe/PbSe interface was found to be 0.043 eV (we use the convention that a positive value indicates that the constituent on the right-hand-side has higher valence band). By fitting measured Hall coefficient and transverse magnetoresistance data,[9] the valence-band offsets for PbTe/PbS has also been estimated to be 0.32 $\pm$0.05 eV. Both are in reasonably good agreement with our calculated results of Fig. 2.

We have also studied the effects of strain on the valence-band offset. We find that for PbTe/PbSe, PbSe/PbS, and PbTe/PbS the valence-band offsets for interfaces coherently strained at $\overline{a}(x=0.5)$ are -0.27, -0.16, and -0.32 eV, respectively. The reason for the sign change with respect to the unstrained case is that when a component is compressed (e.g., PbTe in PbTe/PbSe), its VBM energy goes up due to larger *p*-*s* repulsion. Notice that the transitivity rule observed for unstrained band offsets (Fig. 3) usually does not hold for coherently strained systems.[11]

(e) Why do the band gaps have negative deformation potentials? We have seen that the band gaps in Pb*X* are controlled by *level repulsions*. Since the level repulsion increases when the bond length is shorter, the band gap at *L* will decrease with increasing hydrostatic pressure, thus Pb*X* have negative deformation potentials $dE_g(L)/dP$ (Table II,[21] line 6) and positive-temperature coefficients.[4,22] Note that

TABLE II. Calculated electronic-structure parameters (see text) for PbS, PbSe, and PbTe at their respective experimental lattice constants. Energies are in eV, except for the deformation potentials which are in meV/kbar. Results are compared with available experiment data compiled in Ref. 4.

	PbS		PbSe		PbTe	
Property	Calc.	Expt.	Calc.	Expt.	Calc.	Expt.
$E_g(L)$	0.29	0.29	0.17	0.17	0.19	0.19
$E_g(\Gamma)$	5.97		5.17		3.92	
$\Delta\epsilon(L_{3'c} - L_{2'c})$	1.59		1.43		0.55	
$E_g(L) - E_g^{\mathrm{SR}}(L)$	-0.29		-0.33		-0.62	
$\Delta\epsilon(L_{6^+v} - \Gamma_{8^-v})$	2.01		1.63		1.07	
$dE_g(L)/dP$	-5.24	-9.1	-5.18	-8.6	-4.01	-7.4

TABLE III. Breakdown of the calculated bowing-coefficient for random chalcogenides-alloys (in eV) into ''volume deformation'' (VD), ''charge exchange'' (CE), and ''structural relaxation'' (SR) contributions (see text). b is the total bowing.

System	b_{VD}	b_{CE}	b_{SR}	b
$PbS_{0.5}Se_{0.5}$	0.00	0.00	0.03	0.03
$PbSe_{0.5}Te_{0.5}$	−0.08	−0.06	0.05	−0.09
$PbS_{0.5}Te_{0.5}$	−0.10	−0.04	0.10	−0.04

while the band-edge state L_{6^-c} and L_{6^+v} have different symmetries (hence, they can cross when pressure is applied), the states away from the L point (e.g., Λ_6) have identical symmetries (thus, cannot cross). Therefore, when pressure is applied to PbX, the band gaps will initially decrease, approaching zero at $P=P_c$, and then they will increase. We predict that the pressure coefficient of the band gap will change signs at a critical pressure P_c when E_g vanishes. Using the experimental band gaps and the pressure coefficient given in Table II, we estimate the transition pressure $P_c=32$, 20, and 16 kbar for PbS, PbSe, and PbTe, respectively.

(f) Why is the optical bowing coefficient of the $PbSe_xTe_{1-x}$ alloy negative? We have analyzed b by decomposing it into physically distinct additive-contributions:[23] (1) volume deformation (VD), (2) charge exchange (CE), and (3) structural relaxation (SR). The VD term represents changes in the band gaps due to compression or dilation of the constituents from their individual equilibrium lattice constants to the intermediate alloy value $a(x)$. The CE term is the change in band gaps in bringing together the constituents, both already prepared at $a=a(x)$, thus forming an alloy at $a=a(x)$ with all atoms assumed to be on ideal rocksalt lattice sites (unrelaxed SQS). Finally, the SR term represents the change of band gaps upon passing from the atomically unrelaxed to the relaxed alloy at $a(x)$ (relaxed SQS). By construction, the total bowing is $b\equiv b_{\mathrm{VD}}+b_{\mathrm{CE}}+b_{\mathrm{SR}}$. Table III shows the breakdown of bowing for the three random alloys. We observe the following: (i) by definition, b_{VD} is proportional to the lattice mismatch and to the difference in the deformation potentials between PbX and PbY. Since the magnitude of the deformation potential is reduced in the series PbS→PbSe→PbTe (Table II, line 6), b_{VD} is negative in the alloys. (ii) b_{SR} is positive, partially canceling the effect of volume deformation. The total bowing is thus determined mostly by (iii) b_{CE} which is negative in these systems. In a previous study,[24] the negative bowing in $PbSe_xTe_{1-x}$ was attributed to the reversal of the order of the $L_{3'c}$ and $L_{2'c}$ states in PbTe relative to PbSe, predicted from empirical pseudopotential calculations.[25,13,26] Because of this level reversal, the CBM on one end of the alloy composition traces a line towards a state with energy higher than the CBM on the other end of the alloy composition. Consequently, the CBM of the alloy would be higher in energy than the weighted average, thus $b<0$. However, our self-consistent calculations show that although PbTe has a much smaller energy difference $\Delta\epsilon(L_{3'c}-L_{2'c})$ than PbSe and PbS (Table II, line 3), the level order in all three compounds is the same. We find instead that due to the closeness of the energies of $L_{3'c}$ and $L_{2'c}$ in PbTe, these two states are strongly coupled (through the spin-orbit interaction). This leads to negative b_{CE}, thus to negative total bowing in $PbSe_xTe_{1-x}$. Our calculated $b=-0.09$ eV for $PbSe_xTe_{1-x}$ is in good agreement with experimental data $b\sim-0.1$ eV.[14,15]

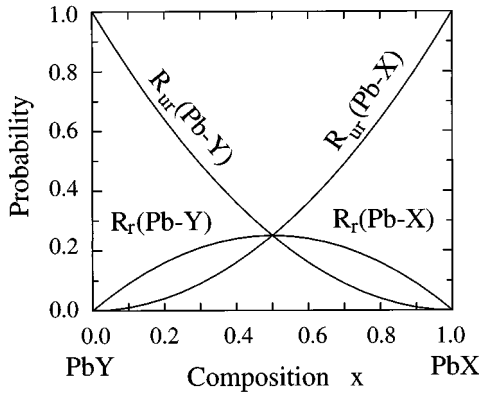

FIG. 4. Calculated probability of finding relaxed and unrelaxed bonds in random rocksalt PbX_xY_{1-x} alloy. The probabilities of finding unrelaxed bonds $R_{\mathrm{ur}}(\mathrm{Pb}-X)$ and $R_{\mathrm{ur}}(\mathrm{Pb}-Y)$ are x^2 and $(1-x)^2$, respectively, while the probabilities of finding the relaxed bonds $R_r(\mathrm{Pb}-X)$ and $R_r(\mathrm{Pb}-Y)$ are $x(1-x)$.

(g) Why does $PbS_{0.2}Te_{0.8}$ show two different Pb-S bond lengths? Atoms in a covalent alloy relax to attain as much as possible ''ideal'' bond lengths $R^0(\mathrm{Pb}-X)$ and $R^0(\mathrm{Pb}-Y)$ and bond angles.[27] Our total energy and force calculations show that in the Pb X_xY_{1-x} alloys energy is lowered primarily by bond-*stretching* relaxation, while the effect of bond-*bending* relaxation on the total energy is small (a consequence of ionicity). Further, we find that bond relaxation occurs here primarily through displacement of the *common* sublattice atom (i.e., Pb). These features are similar to that found in zinc-blende alloys.[27] What is different here is that in the Pb centered ideal X_nY_{6-n} ($n=0$–6) octahedra, since any two cation-anion bonds are either parallel or orthogonal to each other, to first order, displacement of Pb can make only *some* of the bonds $R_r(\mathrm{Pb}-X)$ relax (r) towards their ideal $R^0(\mathrm{Pb}-X)$ values. The remaining bonds $R_{\mathrm{ur}}(\mathrm{Pb}-X)$are ''unrelaxed'' (ur), being closer to the composition-weighted average $R(x)=(1-x)R^0(\mathrm{Pb}-X)+xR^0(\mathrm{Pb}-Y)$. Figure 4 gives our calculated probabilities of finding relaxed and unrelaxed bonds in a random rocksalt alloy. In calculating these probabilities we assume that the mixed anions are located on the ideal fcc sites[28] with lattice constant $a(x)$, and that the Pb atom relaxes only if it simultaneously reduces the bond length of one component and increases the bond length of the other. We see from Fig. 4 that at $x=0.5$, for each anion-cation pair, half of the bonds are relaxed while the other half are unrelaxed. Thus we predict that in lattice-mismatched rocksalt alloy a four-modal bond-length distribution with two bond lengths for each cation-anion pair should exist.

In a recent extended x-ray absorption fine-structure. measurement, Wang and Bunker[16] found that two types of Pb-S bonds exist in Te-rich PbS_xTe_{1-x} alloys, while only one type of Pb-Te bond was observed. To explain this, they suggested that this alloy underwent a ferroelectric transition that leads to some of the S atoms displaced from their ideal fcc sites, moving towards Pb to form short Pb-S bonds. Our results and analysis above, however, suggest that, despite the role

TABLE IV. Calculated formation-energies (in meV/4-atoms) of ordered $(PbX)_n/(PbY)_n$ structures (see ordering direction) and of the random alloy of the same, $x=0.5$ composition.

System direction	CuAu (001)	Y2 (110)	CuPt (111)	Random
Pb_2SSe	49	20	12	20
Pb_2SeTe	153	60	22	56
Pb_2STe	378	151	60	147

played by ferroelectric transition in the system, the bimodal distribution of the Pb-S bonds is an intrinsic behavior of rocksalt alloys. The short Pb-S bonds are the more relaxed ones while the long Pb-S bonds correspond to the more unrelaxed ones. The ratio between the number of relaxed and unrelaxed bond is predicted to be 4 to 1 at $x=0.2$. On the other hand, at small composition x, the relaxed and unrelaxed Pb-Te bonds have similar lengths, hence may not be distinguished in the experimental analysis.[16] Further study is needed to clarify this issue.

(h) Predicted spontaneous CuPt ordering. We have studied the formation energies $\Delta H(\sigma, Pb_2XY) = E(\sigma, Pb_2XY) - [E(PbX) + E(PbY)]$ of several ordered and disordered rocksalt Pb alloys at $x=0.5$. The configurations σ which we have studied are CuAu [(1,1) superlattice along (001) direction], CuPt [(1,1) superlattice along (111) direction], $Y2$ [(2,2) superlattice along (110) direction], and the random alloy (represented by SQS8). The results are shown in Table IV. We find that in general ΔH are positive and increase with the lattice mismatch between the constituents. Furthermore, the ordered CuPt structure, which has the *highest* energy among all short-period superlattices in lattice mismatched *zinc-blende* alloys[29] has the *lowest* energy in rocksalt alloys. This could be understood by noticing that the rocksalt (but not zinc-blende) ordered CuPt structure permits *all* nearest cation-anion bond lengths to attain their respective ideal values with minimum bond bending. Consequently, the formation energy of the rocksalt CuPt structure is much lower than that for the random rocksalt alloy (especially for Pb_2STe). We thus predict that at low temperature, when phase separation is slowed down or even forbidden by kinetic effects, the ordered CuPt structure could be observed in $x=0.5$ bulk alloy. The formation of this CuPt structure is also predicted to transform the alloy into a slightly indirect gap material, with VBM at the L point along the $\langle 111 \rangle$ ordering direction and the CBM at the other L points.

IV. SUMMARY

We have studied the electronic structure of Pb chalcogenides using a self-consistent all-electron method. We find that unlike the zinc-blende semiconductor compounds, the band structures of PbX compound has an occupied Pb s band, which leads to strong-level repulsion at the L point between the Pb s and the anion p states. We have explained the seemingly unrelated electronic-structural anomalies of the Pb chalcogenides using the s-p level repulsion mechanism. We find that bond relaxation in rocksalt alloy is qualitatively different from that in the zinc-blende alloy in that a significant fraction of the bonds do not relax towards their ideal values. We predict that due to the topology of the frustrated octahedral structure, a four-modal bond length distribution is expected in the Pb alloys. Further experimental and theoretical studies are needed to test our predictions.

ACKNOWLEDGMENT

This work was supported by the U.S. DOE/EE, Grant No. DE-AC36-83-CH10093.

[1] H. Zogg, A. Fach, J. John, J. Masek, P. Muller, C. Paglino, and W. Buttler, Opt. Eng. **33**, 1440 (1994).
[2] H. Preier, Appl. Phys. **20**, 189 (1979).
[3] T. K. Chaudhuri, Int. J. Eng. Res. **16**, 481 (1992).
[4] G. Nimtz and B. Schlicht, *Narrow-Gap Semiconductors* (Springer-Verlag, New York, 1985), and references therein.
[5] *Numerical Data and Functional Relationships in Science and Technology*, edited by O. Madelung, M. Schulz, and H. Weiss, Landolt-Börnstein, New Series, Vol. 17, Pt. a (Springer-Verlag, Berlin, 1982).
[6] D. L. Mitchell, E. D. Palik, and J. N. Zemel, in *Physics of Semiconductors: Proceedings of the Seventh International Conference, Paris, 1964*, edited by M. Hulin (Academic, New York, 1964), p. 325.
[7] R. Dalven, Phys. Rev. B **3**, 3359 (1971), and references therein.
[8] E. Grodzicka, W. Dobrowolski, T. Story, Z. Wilamowski, and B. Witkowska, in *Proceedings of the Tenth International Conference on Ternary and Multinary Compounds Stuttgart, Germany, 1995*, edited by H. W. Schock and T. C. Walter (Akademie Verlag, Berlin, 1996).
[9] F. F. Sizov, J. V. Gumenjuk-Sichevskaya, V. V. Tetyorkin, and V. V. Zabudsky, Acta Physica Pol. A **87**, 441 (1995).
[10] S.-H. Wei and A. Zunger, Phys. Rev. B **53**, R 10 457 (1996).
[11] S.-H. Wei and A. Zunger, J. Appl. Phys. **78**, 3846 (1995), and references therein.
[12] A. A. Andreev, J. Phys. C **4**, 50 (1968).
[13] M. Schluter, G. Martinez, and M. L. Cohen, Phys. Rev. B **12**, 650 (1975).
[14] F. E. Faradzhev, Fiz. Tekh. Poluprovodn. **18**, 2104 (1984) [Sov. Phys. Semicond. **18**, 1311 (1984)].
[15] M. V. Valeiko, I. I. Zasavitskii, V. L. Kuznetsov, A. V. Kurganskii, and B. N. Matsonashvili, Fix. Tekh. Poluprovodn. **19**, 627 (1985) [Sov. Phys. Semicond. **19**, 388 (1985)].
[16] Z. Wang and B. A. Bunker, Phys. Rev. B **46**, 11 277 (1992).
[17] J. C. Mikkelsen and J. B. Boyce, Phys. Rev. Lett. **49**, 1412 (1982); Phys. Rev. B **28**, 7130 (1983).
[18] S.-H. Wei and H. Krakauer, Phys. Rev. Lett. **55**, 1200 (1985), and references therein.
[19] J. P. Perdew and A. Zunger, Phys. Rev. B **23**, 5048 (1981).
[20] A. Zunger, S. H. Wei, L. G. Ferreira, and J. E. Bernard, Phys. Rev. Lett. **65**, 353 (1990).
[21] The calculated magnitude of the deformation potentials are about 40% smaller than the experimental values. The underestimation of the deformation potentials results from the LDA's overesti-

mation of the binding energy of the Pb *s* band (similar to the LDA error in the band gap), thus to an underestimation of the *p*-*s* level repulsion. If one adjusts the Pb *s* band to lower binding energy (Refs. 22 and 13), the calculated magnitude of the deformation potential becomes larger.

[22] Y. W. Tsang and M. L. Cohen, Phys. Rev. B **3**, 1254 (1971).

[23] J. E. Bernard and A. Zunger, Phys. Rev. B **36**, 3199 (1987).

[24] A. Jedrzejczak, D. Guillot, and G. Martinez, Phys. Rev. B **17**, 829 (1978).

[25] R. L. Bernick and L. Kleinman, Solid State Commun. **8**, 569 (1970).

[26] G. Martinez, M. Schluter, and M. L. Cohen, Phys. Rev. B **11**, 651 (1975); **11**, 660 (1975).

[27] J. L. Martins and A. Zunger, Phys. Rev. B **30**, 6127 (1984).

[28] In reality, atoms on the mixed sublattice also shift from their ideal fcc sites to reduce the strain energy. See A. Silverman, A. Zunger, R. Kalish, and J. Adler, Phys. Rev. B **51**, 10 795 (1995).

[29] R. G. Dandrea, J. E. Bernard, S.-H. Wei, and A. Zunger, Phys. Rev. B **30**, 6127 (1984).